High electronegativity multi-dipolar electron cyclotron resonance plasma source for etching by negative ions

Stamate, Eugen; Draghici, M.

Published in:
Journal of Applied Physics

Link to article, DOI:
10.1063/1.4704696

Publication date:
2012

Document Version
Publisher's PDF, also known as Version of record

High electronegativity multi-dipolar electron cyclotron resonance plasma source for etching by negative ions

E. Stamate and M. Draghici

Citation: J. Appl. Phys. **111**, 083303 (2012); doi: 10.1063/1.4704696
View online: http://dx.doi.org/10.1063/1.4704696
View Table of Contents: http://jap.aip.org/resource/1/JAPIAU/v111/i8
Published by the American Institute of Physics.

High electronegativity multi-dipolar electron cyclotron resonance plasma source for etching by negative ions

E. Stamate[1,a)] and M. Draghici[2]
[1]*Department of Energy Conversion and Storage, Technical University of Denmark, Frederiksborgvej 399, Roskilde 4000, Denmark*
[2]*Infineon Technologies Austria AG, Siemensstraße 2, Villach 9500, Austria*

(Received 30 January 2012; accepted 12 March 2012; published online 23 April 2012)

A large area plasma source based on 12 multi-dipolar ECR plasma cells arranged in a 3×4 matrix configuration was built and optimized for silicon etching by negative ions. The density ratio of negative ions to electrons has exceeded 300 in Ar/SF_6 gas mixture when a magnetic filter was used to reduce the electron temperature to about 1.2 eV. Mass spectrometry and electrostatic probe were used for plasma diagnostics. The new source is free of density jumps and instabilities and shows a very good stability for plasma potential, and the dominant negative ion species is F^-. The magnetic field in plasma volume is negligible and there is no contamination by filaments. The etching rate by negative ions measured in $Ar/SF_6/O_2$ mixtures was almost similar with that by positive ions reaching 700 nm/min. © *2012 American Institute of Physics*. [http://dx.doi.org/10.1063/1.4704696]

I. INTRODUCTION

Patterning of high-aspect-ratio features with high selectivity, accurate profile, high uniformity, and low damage using plasma etching is an essential technology for micro- and nano-electronic industry.[1–7] So far, only positive ions at low pressure and high plasma densities are used to ensure good anisotropy and high etching rates.[8–19] The continuous decreasing of the node size (now below 100 nm) at an increased devices density bring new challenges that need to be solved, including: charging-induced gate breakdown;[20,21] dependence of the etching rate on the pattern size (low RIE-lag effect[22] or aspect-ratio-dependence etching effect) and on the laid-out pattern density (microloading effect);[23] and handling of new materials such as low-k and high-k.[1] In particular, the notch phenomenon[24] induced by side etching with positive ions deflected by the positive space charge accumulated at the bottom of patterns has pointed to the possibility to reduce the charge build-up effect by etching with negative ions that induce lower charging potentials for similar ion fluxes and ion energy.[23] Moreover, negative ion etching can also bring the advantage of replacing the sulfur-based positive-ion-species (SF_2^+ and SF_3^+) that need to dissociate before releasing F^+, with a process dominated by volatile F^-.[25] The energy balance during neutralization also favors negative ions in terms of low damage etching.[26] Reports on negative ion production and extraction for the purpose of etching include microwaves discharges,[25] pulse-time modulated electron cyclotron resonance (ECR) plasma with low-frequency bias,[23,27] pulsed dc bias locked to the source power modulation on an inductively coupled plasma (ICP) afterglow,[28,29] electron-beam-generated electronegative plasmas,[30] single and dual frequency capacitively coupled plasma,[31] ICP,[32,33] and DC discharge.[34] Despite of these efforts to build large area and reliable plasma sources for negative ion etching yet, there are limitations to be overcome. The electron temperature and plasma density are too high in inductively coupled and surface wave plasmas to sustain a density ratio of negative ion to electron, n_{ni}/n_e, higher than 50 (n_{ni} and n_e are the negative ion and electron densities).[33] Moreover, these types of electronegative discharges are affected by instabilities[35] and mode jumps[33] and cannot operate well at low pressures, favorable for large negative ion production. Conventional ECR or helicon plasma sources are using magnetic structures that add an undesirable magnetic field in the plasma volume. A $n_{ni}/n_e > 500$ was reported in DC discharges when a transversal magnetic filter was used to reduce the electron temperature.[34] However, filament discharges are incompatible with most of the equipments used for micro- and nanoelectronic industry. Recently, a new type of ECR plasma source was build, namely, the multi-dipolar ECR,[36–38] which allows one to produce an easy scalable plasma source in various configurations, free of magnetic field in plasma volume, operating even below 10 mTorr. From the point of view of industrial applications, a negative ion plasma source that can provide the following characteristics is desirable: no contamination by filaments, no density jumps; negligible magnetic field in plasma volume; a density ratio of negative ion to electron higher than 50 (as to make it possible to bias the substrate positively without affecting the plasma potential, V_{pl}, and to avoid overheating by electrons[33,34]); stable operation at low pressure with no plasma potential drift;[34] good controllability of ion species and high etching rates.

This work reports on the optimization and diagnostics of a multi-dipolar ECR plasma source in terms of negative ion production and high speed etching by negative ions. Experiments are performed in Ar/SF_6 and $Ar/SF_6/O_2$ gas mixtures and plasma parameters are characterized by mass spectrometry and electrostatic probe.

II. EXPERIMENTAL

A schematic illustration of the experimental setup is presented in Fig. 1(a). A 3×4 matrix configuration of 12 individual multi-dipolar ECR plasma cells produced by Boreal

a)Email: eust@dtu.dk.

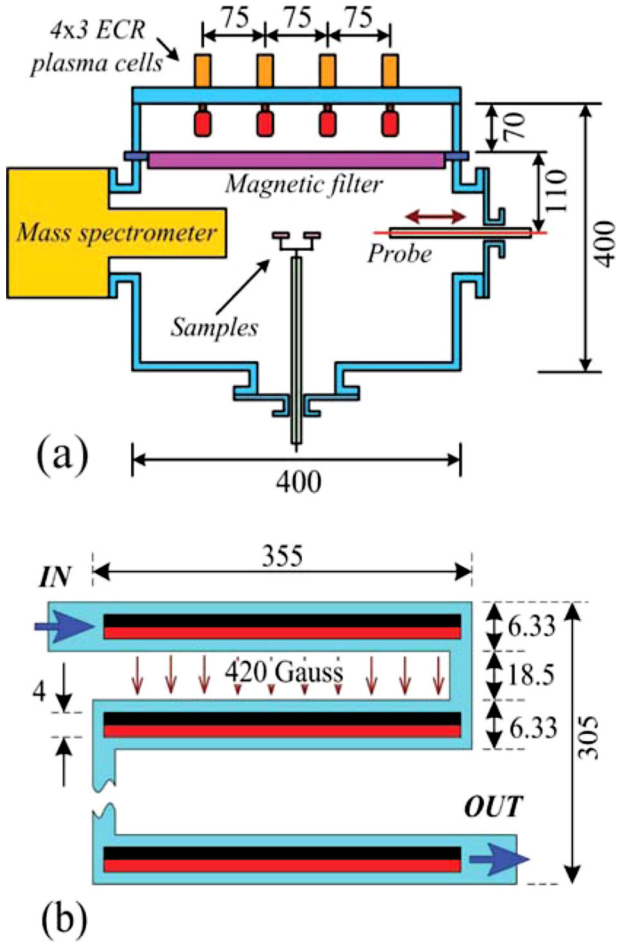

FIG. 1. (a) A schematic illustration of the experimental setup (b) details of the water cooled magnetic filter.

Plasma® is mounted at the top of a cubic chamber ($400 \times 400 \times 400$ mm) with a distance between cells of 75 mm. The microwave power from a 2 kW generator at 2.45 GHz (Sairem®) is divided in 12 channels, so that the power injected into each cell can be adjusted independently, allowing a good controllability of the uniformity profile.[36] Each ECR cell includes a water cooled permanent magnet that provides a localized magnetic field of 875 Gauss necessary for electron cyclotron resonance. A water cooled magnetic filter (see Fig. 1(b)) made of permanent magnets (4 mm in diameter, 10 mm in length, and 2000 Gauss at the surface) magnetized on sides and inserted in a 6.33 mm pipe welded in 13 parallel lines situated 25 mm apart is used to reduce the electron temperature, T_e, by increasing the diffusion time of electrons from the plasma production region to the processing region.[39] The filter is placed 70 mm below the top plate supporting the plasma cells. The penetration of the magnetic field in plasma volume is negligible (less than 50 Gauss) at a distance larger than 5 cm form the filter. A Hiden® mass spectrometer and a cylindrical probe (10 mm long, 0.2 mm in diameter made of platinum) are placed on opposite laterals sides at 110 mm below the magnetic filter. A holder that can host 8 samples (1 cm^2, made of *n*-type silicon, of orientation ⟨100⟩, doped with phosphorus with a resistivity lower than 0.02 Ω cm) and can expose them one by one to similar plasma conditions through the controllable rotation of a mask (4×4 mm) is placed at the same lineament with the probe and the mass spectrometer. The etching rates are estimated using a Veeco® deck tack profiler. The "test function" method[39,40] in the approximation of bi-Maxwellian electron energy distribution function (EEDF) is used to extract plasma parameters from current-voltage probe characteristics including positive ion, negative ion, bulk electron and hot electron densities (n_x), and temperatures (T_x), where for notation, the subscript *x* is replaced with *i* for positive ions, *ni* for negative ions, *eb* for bulk electrons, and *eh* for hot electrons.[41] The total electron density, n_e, is defined as $n_e = n_{eb} + n_{eh}$. The n_i is calculated from the ion saturation region of the probe characteristic using the orbital motion limited model under the approximation that $T_{eb}/T_i = 10$.[41] Effective electron temperature, T_{eff}, is also calculated in negative ion free plasma (Ar discharge) by integrating the EEDF.[42] The error range for measuring plasma parameters from probe characteristics was estimated to be below 10%. Special care was taken regarding surface contamination during probe measurements.[43,44]

III. RESULTS AND DISCUSSION

The T_{eff} and n_e measured with (dashed line) and without (continuous line) the magnetic filter as a function of pressure, *p*, are presented in Fig. 2 for 500 W discharge power, *P*, in Ar gas. The probe was located 11 cm below the filter at the center of the chamber. Besides a large range of operation not accessible for ICP discharges (0.1 up to 10 mTorr), one can notice the effectiveness of the magnetic filter to reduce T_{eff} from more than 2 eV to about 1.2 eV for $p > 2$ mTorr, a value that gives the largest cross section for F^- formation. The n_i and V_{pl} as a function of *P* up to 1000 W are presented in Fig. 3 for 0.5 and 5 mTorr. Smooth operation with no mode jumps, $n_i > 10^{16}$ m^{-3} and $V_{pl} \approx 4$ V was obtained for 5 mTorr, while lower pressures resulted in $V_{pl} > 10$ V and lower densities. The n_{ni}/n_e and n_i at three different pressures (1, 5, and 10 mTorr) are shown in Fig. 4 as a function of *P* in (a), and SF_6 flow in (b) for $P = 500$ W and Ar flow of 1 sccm. The very large difference in electronegativity with n_{ni}/n_e ranging from about 20 at 1 mTorr up to 300 at 10 mTorr is the results of a lower T_e at higher pressures, where the electron thermalization by collisions in plasma volume (almost free of magnetic field) is furthermore

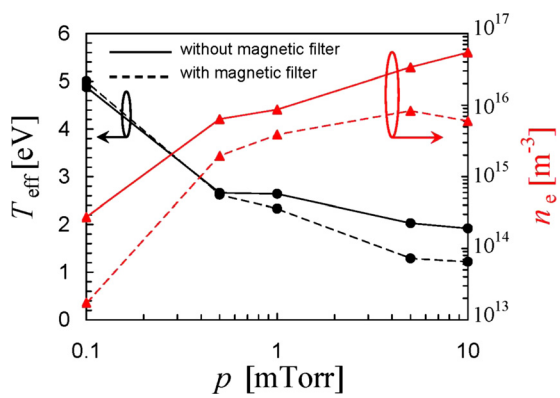

FIG. 2. T_{eff} and n_e measured with (dashed line) and without (continuous line) the magnetic filter as a function of pressure, for 500 W in Ar gas.

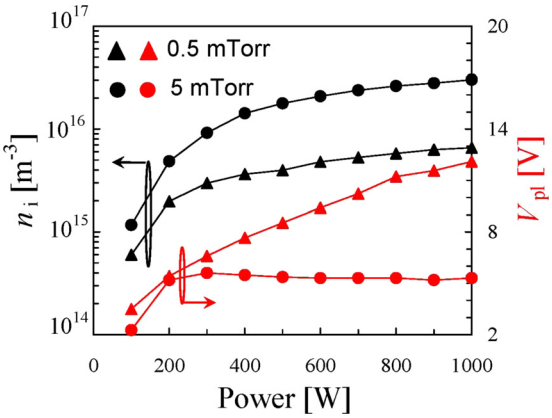

FIG. 3. n_i and V_{pl} as a function of P up to 1000 W for 0.5 and 5 mTorr.

enhanced by the presence of the magnetic filter, as shown in Fig. 2. A $n_{ni}/n_e > 50$ was obtained in a pressure range from 5 to 10 mTorr and $200 < P < 1000$ W for SF_6 flows larger than 0.2 sccm and Ar flow of 1 sccm. A big concern for highly electronegative plasma sources aimed for applications is the V_{pl} drift observed both in DC and ICP discharges.[33,34] The V_{pl} as a function of time is shown in Fig. 5(a) with squares for 1 sccm and circles for 2 sccm of SF_6 flow, while keeping the Ar flow at 1 sccm. Besides a $V_{pl} \sim 0$ V that is advantageous for low damage processing, one can see an almost negligible drift for V_{pl}. The n_{ni}/n_e and n_i corresponding to data in Fig. 5(a) are presented in Fig. 5(b) and show the same stability in time as V_{pl}. Typical electron energy probability function (EEPF) tracks are shown in Fig. 6 as function

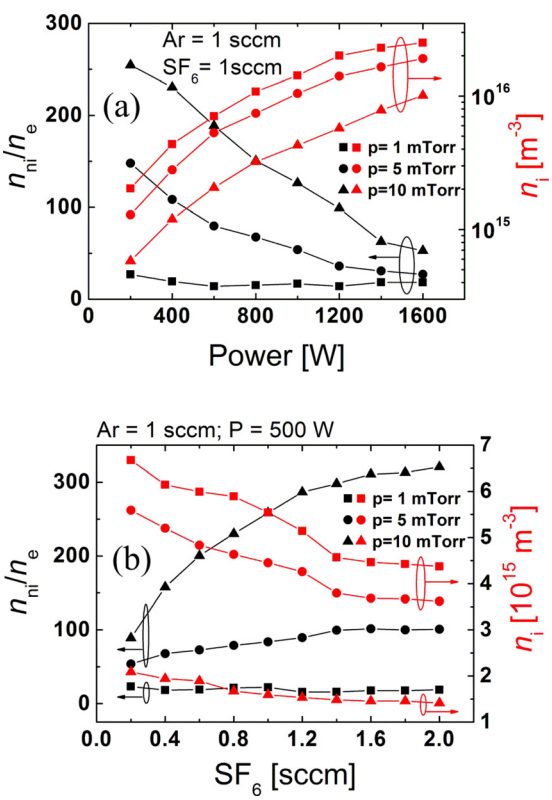

FIG. 4. n_{ni}/n_e and n_i at three different pressures (1, 5, and 10 mTorr) as a function of (a) power and (b) SF_6 flow, for $P = 500$ W, and Ar flow of 1 sccm.

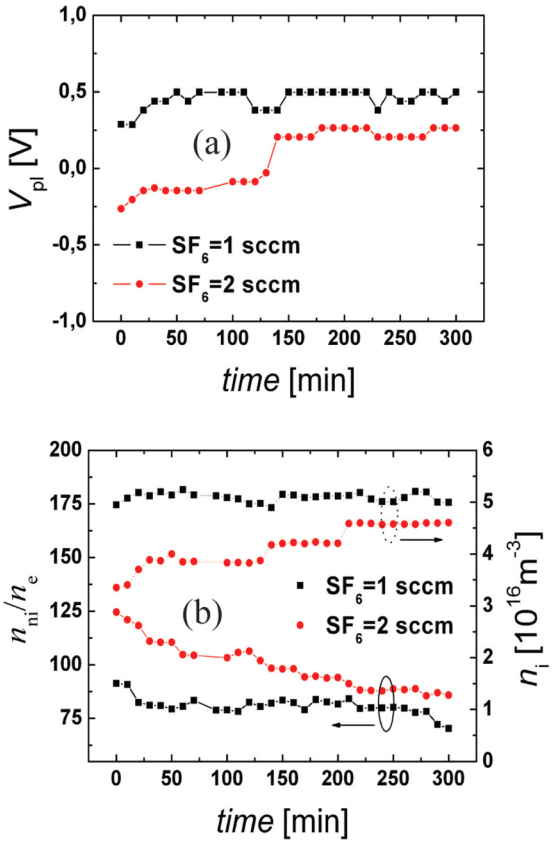

FIG. 5. (a) V_{pl} as a function of time with squares for 1 sccm and circles for 2 sccm of SF_6 flow while keeping the Ar flow at 1 sccm; (b) n_{ni}/n_e and n_i as a function of time corresponding to data presented in (a).

of SF_6 flow for $P = 500$ W, $p = 5$ mTorr, and 1 sccm Ar flow, with a clear evidence for a transition to bi-Maxwellian EEPF at larger n_{ni}/n_e. A similar behavior was previously reported in DC and ICP discharges and it is associated with a depletion of low energetic electrons involved in negative ion formation.[39,41] The uniformity of plasma parameters (V_{pl}, n_i, T_{eff}, and n_{ni}/n_e) was investigated by shifting the probe under the magnetic filter for 36 cm, resulting in deviations from center to the edge below 5%, where no special care was considered for tuning the ECR plasma cells in order to further improve the uniformity.

The amplitude of the mass peaks by mass spectrometry are presented as a function of SF_6 flow in Fig. 7(a) for positive ions and (b) for negative ions, for $P = 500$ W, $p = 5$ mTorr, and Ar flow of 1 sccm. While up to 6 positive ion species were detected (F^+, S^+, SF^+, SF_2^+, SF_3^+, and SF_5^+), the negative ion spectrum was dominated by F^- with considerably lower concentrations of SF_5^- and SF_6^-. The same behavior was observed for p ranging from 1 up to 10 mTorr and for discharge powers below 1600 W. This result is well correlated with the fact that SF_5^- and SF_6^- are formed for $T_e \leq 0.7$ eV while F^- formation peaks around 1 eV.

We demonstrated recently that it is possible to bias a large electrode in a electronegative discharge up to several hundred volts without elevating V_{pl} or igniting a glow (for smaller electrodes) as long as $n_{ni}/n_e > 50$.[33,34] As shown in Fig. 4, this condition is satisfied for $p \geq 5$ mTorr and $P \leq 1500$ W. This high electronegative regime is essential

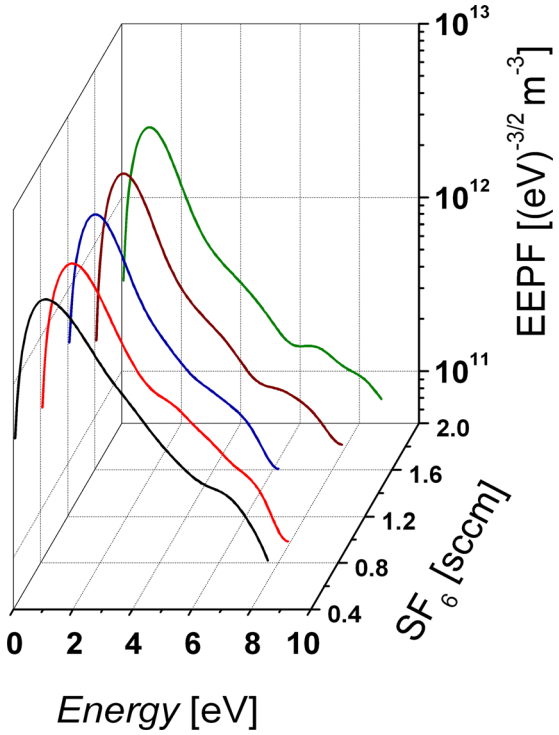

FIG. 6. Typical electron energy probability function tracks as function of SF_6 flow for $P = 500$ W, $p = 5$ mTorr, and 1 sccm Ar flow.

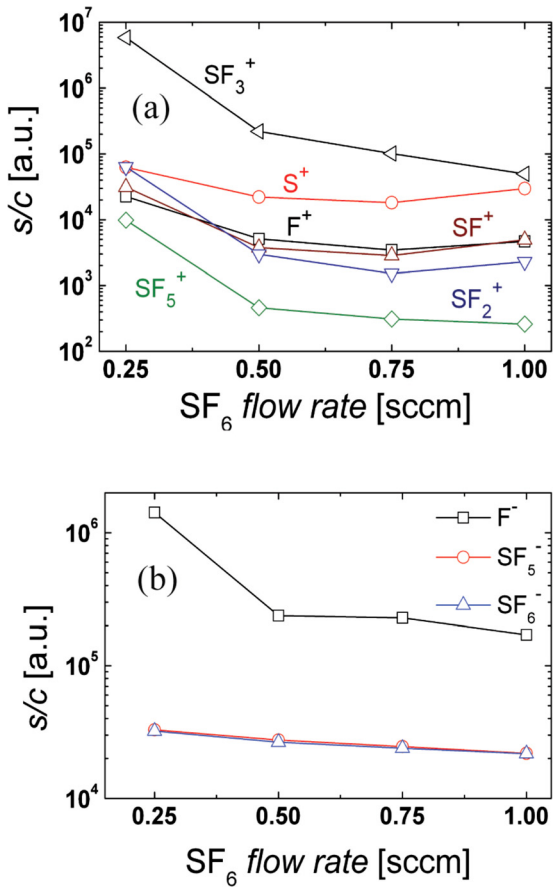

FIG. 7. The amplitude of the mass peaks by mass spectrometry as a function of SF_6 flow (a) for positive ions and (b) for negative ions, where $P = 500$ W, $p = 5$ mTorr, and Ar flow of 1 sccm.

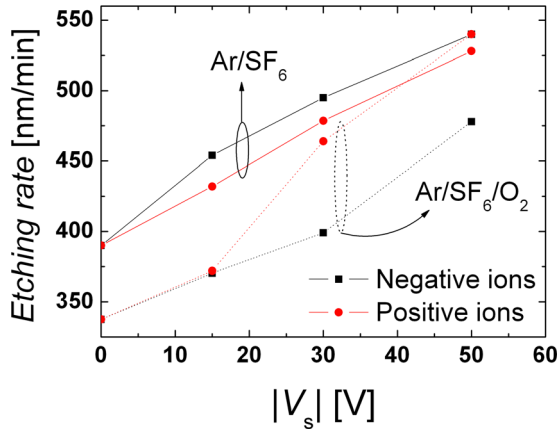

FIG. 8. Etching rates by positive and negative ions as a function of the substrate bias, $|V_s|$, with continuous lines for Ar/SF_6 (Ar: 1 sccm and SF_6: 1 sccm) and dashed lines for $Ar/SF_6/O_2$ gas mixtures (Ar: 1 sccm, SF_6: 1 sccm, and O_2: 0.5 sccm), where $P = 1000$ W and $p = 5$ mTorr.

for the ability to perform negative ion etching under controllable ion energy, anisotropy, and reduced heat flux by electrons. Ar/SF_6 is a widely used gas mixture for etching, in which a small amount of O_2 can be added to promote the formation of a passivation layer that improves the verticality of the etching profile.[1] Etching rates by positive and negative ions as a function of the substrate bias, $|V_s| = |V - V_{pl}|$, where V is the applied bias with respect to the ground, $P = 1000$ W, and $p = 5$ mTorr are presented in Fig. 8 with continuous lines for Ar/SF_6 (Ar: 1 sccm and SF_6: 1 sccm) and dashed lines for $Ar/SF_6/O_2$ gas mixtures (Ar: 1 sccm, SF_6: 1 sccm, and O_2: 0.5 sccm). The etching rates in Ar/SF_6 increased from 375 nm/min only by radicals ($|V_s| = 0$) to about 540 nm/min for $|V_s| = 50$ V for both positive and negative ions. Increasing $|V_s|$ to 100 V and P to 1500 W, we could measure an etching rate of more than 700 nm/min with a difference of about 30–50 nm/min in favor of positive ions as shown in Fig. 9, where the etching rate as a function of P is shown with and without O_2 (Ar: 1sccm, SF_6: 1 sccm, and O_2: 0.5 sccm). A similar trend of lower rates in the presence of O_2 as shown in Fig. 8 was also confirmed in Fig. 9.

Surface roughness is an important parameter for etching patterns below 100 nm and previous results in DC and ICP

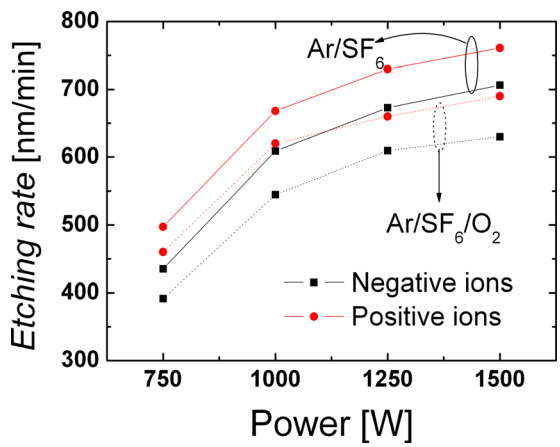

FIG. 9. The etching rate with and without O_2 as a function of P for Ar: 1 sccm, SF_6: 1 sccm, and O_2: 0.5 sccm.

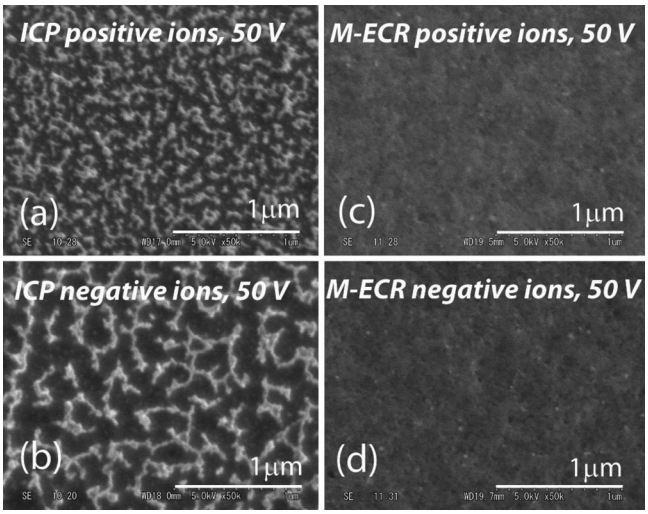

FIG. 10. Surface morphology by SEM after etching for $|V_s| = 50$ V by ICP (see Ref. 33) with (a) positive ions [97 nm] and (b) negative ions [74 nm] and by the ECR plasma source introduced in this work with (c) positive ions [36 nm] and (d) negative ions [28 nm], where $p = 5$ mTorr, $P = 1000$ W, Ar: 1 sccm, SF_6: 1 sccm. Values in square brackets correspond to the root-mean-square measured by AFM using SPIP software.

(Refs. 33 and 34) have shown the formation of self patterning associated with sticking, deposition of sulfur-bearing polymers, or micromasking.[15,45–47] For comparison, surface morphology by scanning electron microscopy (SEM) after etching are shown in Fig. 10 for $|V_s| = 50$ V by ICP (Ref. 33) with (a) positive ions and (b) negative ions and by the ECR plasma source introduced in this work (M-ECR) with (c) positive ions and (d) negative ions ($p = 5$ mTorr, $P = 1000$ W, Ar:1 sccm, and SF_6: 1 sccm). While further investigations are necessary to clarify this difference, it is evident that M-ECR shows a smoother surface without well defined structure as observed in ICP.[33]

IV. CONCLUSIONS

A multi-dipolar ECR plasma source was optimized for negative ion production and tested for etching of silicon in $Ar/SF_6/O_2$ gas mixture under different parameters. The new plasma source included 12 ECR cells arranged in a 3×4 matrix configuration (each cell can be controlled independently) and a transversal magnetic filter that reduced the electron temperature to enhance negative ion production. Over all, the source showed the following advantages: n_{ni}/n_e exceeded 50 in a favorable range of pressure and power, no density jumps or instabilities, scalable processing area by changing the matrix configuration, plasma potential close to 0 V with no drift, F^- as dominant negative ion species, etching rates above 500 nm/min, no magnetic field in plasma volume, and no contamination by filaments. The source is also suitable for basic studies of electronegative discharges and other plasma processing applications including, three-dimensional plasma-sheath-lenses,[48,49] plasma immersion negative ion implantation,[26] and negative ion or neutral beam extraction.[32]

ACKNOWLEDGMENTS

The authors express their gratitude for valuable support to Professor A. Lacoste and Dr. J. Pelletier, Centre de Recherche Plasmas-Matériaux Nanostructures, Grenoble and Dr. J.-L. Delastre (Boreal Plasma, France).

[1]H. Abe, M. Yoneda, and N. Fujiwara, Jpn. J. Appl. Phys., Part 1 **47**, 1435 (2008).
[2]E. L. Hu and R. E. Howard, Appl. Phys. Lett. **37**, 1022 (1980).
[3]C. Pomot, B. Mahi, B. Petit, Y. Arnal, and J. Pelletier, J. Vac. Sci. Technol. B **4**, 1 (1986).
[4]R. H. Burton, R. A. Gottscho, and G. Smolinsky, in *Dry Etching for Microelectronics*, edited by R. A. Powell (Elsevier, New York, 1984), p. 79.
[5]S. J. Pearton, Mater. Sci. Eng. B **10**, 187 (1991).
[6]T. Tatsumi, Appl. Surf. Sci. **253**, 6716 (2007).
[7]D. T. Tran, T. A. Grotjohn, D. K. Reinhard, and J. Asmussen, Diamond Relat. Mater. **17**, 717 (2008).
[8]S. A. McAuley, H. Ashraf, L. Atabo, A. Chambers, S. Hall, J. Hopkins, and G. Nicholls, J. Phys. D: Appl. Phys. **34**, 2769 (2001).
[9]S. Saloum, M. Akel, and B. Alkhaled, J. Phys. D: Appl. Phys. **42**, 175206 (2009).
[10]R. A. Morgan, *Plasma Etching in Semiconductor Fabrication* (Elsevier, Amsterdam, 1985).
[11]T. Sugano, *Application of Plasma Processes to VSLI Technology*, (Wiley-Interscience, New York, 1985).
[12]A. Picard and G. Turban, Plasma Chem. Plasma Process. **5**, 333 (1985).
[13]Y. B. Hahn, S. J. Pearton, H. Cho, and K. P.Lee, Mater. Sci. Eng. B **79**, 20 (2001).
[14]L. Rolland, M.-C. Peignon, Ch. Cardinaud, and G. Turban, Microelectron. Eng. **53**, 359 (2000).
[15]E. Gogolides, C. Boukouras, G. Kokkoris, O. Brani, A. Tserepi, and V. Constantoudis, Microelectron. Eng. **73–74**, 312 (2004).
[16]L. Stafford, J. Margot, M. Chaker, and S. J.Pearton, Appl. Phys. Lett. **87**, 071502 (2005).
[17]J.-P. Booth, C. S. Corr, G. A Curley, J. Jolly, and J. Guillon, Appl. Phys. Lett. **88**, 151502 (2006).
[18]L. Lallement, A. Rhallabi, C. Cardinaud, M. C. Piegnon-Fernandez, and L. L. Alves, Plasma Sources Sci. Technol. **18**, 025001 (2009).
[19]S. Saloum, M. Akel, and B. Alkhaled, J. Phys. D: Appl. Phys. **42**, 175206 (2009).
[20]N. Fujiwara, T. Maruyama, M. Yoneda, K. Tsukamoto, and T. Banjo, Jpn. J. Appl. Phys. Part 1 **33**, 2164 (1994).
[21]N. Fujiwara, T. Maruyama, and M. Yoneda, Jpn. J. Appl. Phys., Part 1 **34**, 2095 (1995).
[22]R. A. Gottscho, C. W. Jurgensen, and D. J. Vitkavage, J. Vac. Sci. Technol. B **10**, 2133 (1992).
[23]H. Otake and S. Samukawa, Appl. Phys. Lett. **68**, 2416 (1996).
[24]M. Yoneda, T. Maruyama, and N. Fujiwara, J. Vac. Sci. Technol. B **12**, 3363 (1994).
[25]H. Shindo, Y. Sawa, and Y. Horiike, Jpn. J. Appl. Phys., Part 1 **34**, L925 (1995).
[26]J. Ishikawa, Rev. Sci. Instrum. **71**, 1036 (2000).
[27]O. Fukumasa and M. Matsumori, Rev. Sci. Instrum. **71**, 935 (2000).
[28]S. K. Kanakasabapathy, M. Khater, and L. Overzet, Appl. Phys. Lett. **79**, 1769 (2001).
[29]S. K. Kanakasabapathy, L. Overzet, V. Midha, and D. Economou, Appl. Phys. Lett. **78**, 22 (2001).
[30]S. G. Walton, D. Leonhardt, R. F. Fernsler, and R. A.Meger, Appl. Phys. Lett. **81**. 987 (2002).
[31]G. A. Curley, D. Maric, J.-P. Booth, C. S. Corr, P. Chabert, and J. Guillon, Plasma Sources Sci. Technol. **16**, S87 (2007).
[32]O. V. Voziy and G. Y. Yeom, Appl. Phys. Lett. **94**, 231502 (2009).
[33]M. Draghici and E. Stamate, J. Appl. Phys. **107**, 123304 (2010).
[34]M. Draghici and E. Stamate, J. Appl. Phys. D: Appl. Phys. **43**, 155205 (2010).
[35]P. Chabert, A. Lichtenberg, M. Liberman, and A. Marakhtanov, Plasma Sources Sci. Technol. **10**, 478 (2001).
[36]A. Lacoste, T. Lagarde, S. Béchu, Y. Arnal, and J. Pelletier, Plasma Sources Sci. Technol. **11**, 407 (2002).
[37]S. Béchu, O. Maulat, Y. Arnal, D. Vempaire, A. Lacoste, and J. Pelletier, Surf. Coat. Technol. **186**, 170 (2004).
[38]L. Latrasse, A. Lacoste, A. Bès, and J. Pelletier, Plasma Sources Sci. Technol. **16**, 7 (2007).
[39]E. Stamate and K. Ohe, J. Appl. Phys. **84**, 2450 (1998).
[40]E. Stamate, G. Popa, and K. Ohe, Rev. Sci. Instrum. **70**, 153 (1999).

[41]E. Stamate and K. Ohe, J. Appl. Phys. **89**, 2058 (2001).
[42]M. A. Lieberman and A. J. Lichtenberg, *Principles of Plasma Discharges and Materials Processing* (Wiley, New York, 1994).
[43]E. Stamate and K. Ohe, Appl. Phys. Lett. **78**, 153 (2001).
[44]E. Stamate and K. Ohe, J. Vac. Sci. Technol. A **20**, 661 (2002).
[45]E. Stamate, H. Sugai, and K. Ohe, Appl. Phys. Lett. **80**, 3066 (2002).
[46]J. Drotar. Y.-P. Zhao, T.-M. Lu, and G.-C. Wang, Phys. Rev. B **61**, 3012 (2000).
[47]G. Boulousis, V. Constantoudis, G. Kokkoris, and E. Gogolides, Nanotechnology **19**, 255301 (2008).
[48]E. Stamate and H. Sugai, Phys. Rev. Lett. **94**, 125004 (2005).
[49]E. Stamate and H. Sugai, Phys. Rev. E **72**, 036407 (2005).